

COMPARISON AND EXPERIENCES WITH FIELD TECHNIQUES TO MEASURE CRITICAL SHEAR STRESS AND ERODIBILITY OF COHESIVE DEPOSITS

Andrew Simon, Research Geologist, USDA-ARS, National Sedimentation Laboratory, Oxford, MS, andrew.simon@ars.usda.gov; Robert E. Thomas, Postdoctoral Research Associate, Dept. of Civil and Environmental Engineering, University of Tennessee, Knoxville, TN; rob.thomas@ars.usda.gov; Lauren Klimetz, Research Associate, Dept. of Civil and Environmental Engineering, University of Tennessee, Knoxville, TN lauren.klimetz@ars.usda.gov

Abstract Predicting the erosion of cohesive materials has long been a challenging task owing to the difficulty in determining the controlling forces that resist entrainment by hydraulic stress, and in characterizing the inherent variability of a cohesive deposit. Whereas entrainment of non-cohesive materials is a function of factors such as particle size, shape, weight and degree of hiding or exposure, the resistance of cohesive materials is controlled by the nature and strength of the inter-particle bonds. Still, accurately quantifying entrainment thresholds (critical shear stress) and erosion rates (erodibility coefficient) are crucial for predicting the stability of earthen structures as well as rates of channel adjustment. In recent years, three field instruments have been developed to indirectly measure the critical shear stress (τ_c) of cohesive deposits *in situ*; two jet-test devices and the cohesive strength meter (CSM). The jet devices also provide an indirect measurement of the erodibility coefficient (k) and measure depth of erosion at fixed intervals. Erosion parameters are then calculated by regression. The CSM measures and records light transmission of the jetted fluid also at fixed intervals. τ_c is obtained by plotting the data and obtaining the shear-stress value at 90% light transmission. This study brings together results of about 1,100 jet tests performed on fine-grained alluvial materials in 16 states across the United States, as well as comparison tests conducted in one Oregon basin with the original jet device, a “mini” jet device and the CSM.

Results show that for each watershed tested, the general inverse-power form of the relation between τ_c and k documented by Hanson and Simon (2001) from tests in Iowa, Mississippi and Nebraska were maintained. Data scatter increases dramatically with decreasing τ_c to roughly 0.1 Pa. At τ_c less than 0.1 Pa, the relation breaks down for all testing locations and there is either (1) no discernable relation or (2) k attains a roughly constant, maximum value. These results imply that k does not vary by an inverse power function under conditions of very high excess shear stress (in the range of 100 to 1,000), but reaches a maximum value as a function of the nature of the eroding materials. For example, at τ_c less than 0.1 Pa (high excess shear stress), median k ranged from 0.28 $\text{cm}^3\text{N}^{-1}\text{s}^{-1}$ for the relatively resistant streambeds of the Yalobusha River, MS to 33.4 $\text{cm}^3\text{N}^{-1}\text{s}^{-1}$ for the sandier alluvium of the Upper Truckee River, CA. Relations calculated in this study were, therefore, truncated at $\tau_c = 0.1$. Combining all available data in this way gives a steeper regression with a higher coefficient than the original published by (Hanson and Simon, 2001). Whereas the original relation was: $k = 0.2 \tau_c^{-0.5}$ ($r^2 = 0.64$), where k is in $\text{cm}^3\text{N}^{-1}\text{s}^{-1}$ and τ_c is in Pa, this study shows that $k = 1.6 \tau_c^{-0.826}$ ($r^2 = 0.62$). Data scatter, however, is still large with 95% prediction limits covering two orders of magnitude for a given τ_c . Relations calculated for each watershed had exponents ranging from -0.11 to -1.0 and coefficients ranging from 0.25 to 6.1.

Data were filtered by non-dimensional time (T^*) to reduce uncertainty in the relations by including only those tests that had attained a threshold value of the equilibrium scour depth. Filtering by a T^* -value of 0.25 was shown to produce the highest r^2 value, reduce uncertainty in prediction limits and represent 70-75% of the equilibrium scour depth over a range of critical shear stress to applied shear stress ratios.

INTRODUCTION

Streambed Erosion by Hydraulic Shear Whether sediment is entrained by a moving fluid depends on both the properties of the fluid (i.e. its density, viscosity and velocity) and the physical properties of the sediment, such as its size, shape, density and arrangement (Knighton, 1998). A basic distinction exists between the entrainment of non-cohesive sediment (usually coarse silt, sand, gravel and boulders or cobbles) and cohesive sediments, because the entrainment of the latter is complicated by the presence of cohesion (Knighton, 1998). In both cases, most approaches to sediment transport have relied upon the concept of a critical value of some parameter. The present paper utilizes the applied shear stress, τ_o as the independent variable.

Mechanisms of Cohesive Sediment Erosion Mechanistically, the detachment and erosion of cohesive (silt- and clay-sized) material by gravity and/or flowing water is controlled by a variety of physical, electrical, and chemical forces. Identification of all of these forces and the role they play in determining detachment, incipient motion, and erodibility, of cohesive materials is incomplete and still relatively poorly understood (Winterwerp and van Kesteren, 2004). Assessing the erosion resistance of cohesive materials by flowing water is complex due to the difficulties in characterizing the strength of the electro-chemical bonds that define the resistance of cohesive materials. The many studies that have been conducted on cohesive materials have observed that numerous soil properties influence erosion resistance including antecedent moisture, clay mineralogy and proportion, density, soil structure, organic content, as well as pore and water chemistry (Grissinger, 1982). For example, Arulanandan (1975) described how the erodibility of a soil decreases with increasing salt concentration of the eroding fluid, inducing weakening of inter-particle bonds. Kelly and Gularte (1981) showed that for cohesive sediments, increasing temperature increases erosion rates, particularly at low salinity, while at high salinity, there is less of an effect on erosion.

Cohesive materials can be eroded in three contrasting ways (Mehta 1991): (1) surface erosion of bed aggregates; (2) mass erosion of the bed; and (3) entrainment of fluid mud. Partheniades (1965) showed that clay resistance to erosion seemed to be independent of the macroscopic shear strength of the bed, provided that the bed shear stresses did not exceed the macroscopic shear strength of the material. Once the bed shear stress exceeds some critical value, then following Ariathurai and Arulanandan (1978) the rate of erosion, ε , of cohesive materials can be predicted by:

$$\begin{aligned} \varepsilon &= k_d \left(\frac{\tau_o}{\tau_c} - 1 \right)^a && \text{(for } \tau_o > \tau_c) \\ \varepsilon &= 0 && \text{(for } \tau_o \leq \tau_c) \end{aligned} \quad (1)$$

where k_d = erosion rate coefficient (m s^{-1}), τ_o = bed shear stress (Pa), τ_c = critical shear stress (Pa), and a = exponent assumed to equal 1.0. Equation 1 may also be written as (Partheniades, 1965):

$$\begin{aligned} \varepsilon &= \frac{k_d}{\tau_c} (\tau_o - \tau_c) = k (\tau_o - \tau_c) && \text{(for } \tau_o > \tau_c) \\ \varepsilon &= 0 && \text{(for } \tau_o \leq \tau_c) \end{aligned} \quad (2)$$

where k = erodibility coefficient ($\text{m}^3\text{N}^{-1}\text{s}^{-1}$). Note, however, that this simple approach does not differentiate between the different modes of erosion.

INSTRUMENTS AND TECHNIQUES FOR *IN SITU* MEASUREMENT OF EROSION OF COHESIVE DEPOSITS

Jet-Test Device A submerged jet-test was developed by the Agricultural Research Service (Hanson, 1990; Figure 1) for testing the *in situ* erodibility of surface materials (ASTM, 1995). This device was developed based on knowledge of the hydraulic characteristics of a submerged jet and the characteristics of soil-material erodibility. In an attempt to remove empiricism and to obtain direct measurements of τ_c and k , Hanson and Cook (1997) developed analytical procedures for determining soil k based on the diffusion principles of a submerged circular jet and the corresponding scour produced by the jet. These procedures are based on analytical techniques developed by Stein et al. (1993) for a planar jet at an overfall and extended by Stein and Nett (1997). Stein and Nett (1997) validated this approach in the laboratory using six different soil types.

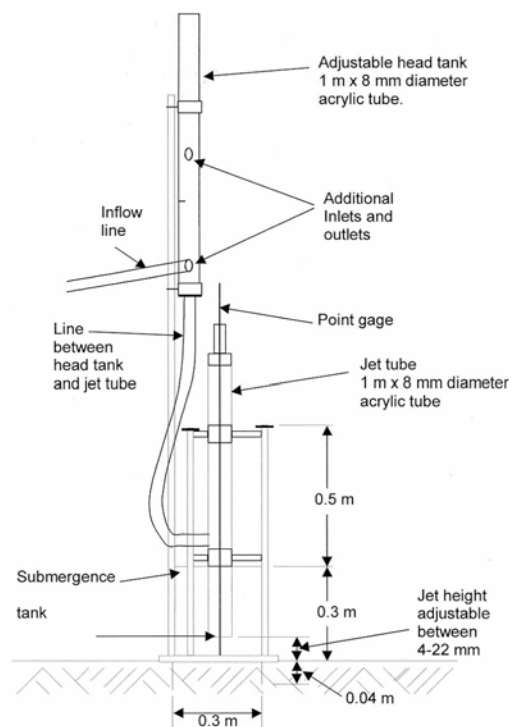


Figure 1 Schematic of jet-test device (from Hanson and Simon, 2001).

As the scour depth increases with time, the applied shear stress decreases due to increasing dissipation of jet energy within the plunge pool. Detachment rate is initially high and asymptotically approaches zero as shear stress approaches the critical shear stress of the bed material. The difficulty in determining equilibrium scour depth is that the length of time required to reach equilibrium can be large. Blaisdell et al. (1981) observed during studies on pipe outlets that scour in cohesionless sands continued to progress even after 14 months. They developed a function to compute the equilibrium scour depth that assumes that the relation between scour and time follows a logarithmic-hyperbolic function. Fitting the jet-test data to the logarithmic-hyperbolic method described in Hanson and Cook (1997) can predetermine τ_c . k is then estimated by curve-fitting measured values of scour depth versus time and minimizing the error of the measured time versus the predicted time. Both k and τ_c are treated as soil properties and the former does not generally correlate well with standard soil mechanical indices such as Atterberg limits. Instead, k is dependent on the physio-chemical parameters that determine the inter-particle forces characteristic of cohesive sediment (Parchure and Mehta, 1985; Mehta, 1991).

“Mini” Jet-Test Device At the request of the National Sedimentation Laboratory, a miniature version of the jet-test device was developed in 2008 by Dr. Greg Hanson of the Agricultural Research Service in Stillwater, OK (Figure 2). The mini-jet apparatus consists of an electric submersible 60 liters/second pump powered by a portable A/C generator, a scaled-down 0.12 m-diameter submergence tank with an integrated, rotatable 3.18 mm-diameter nozzle, depth gauge, and delivery hoses.

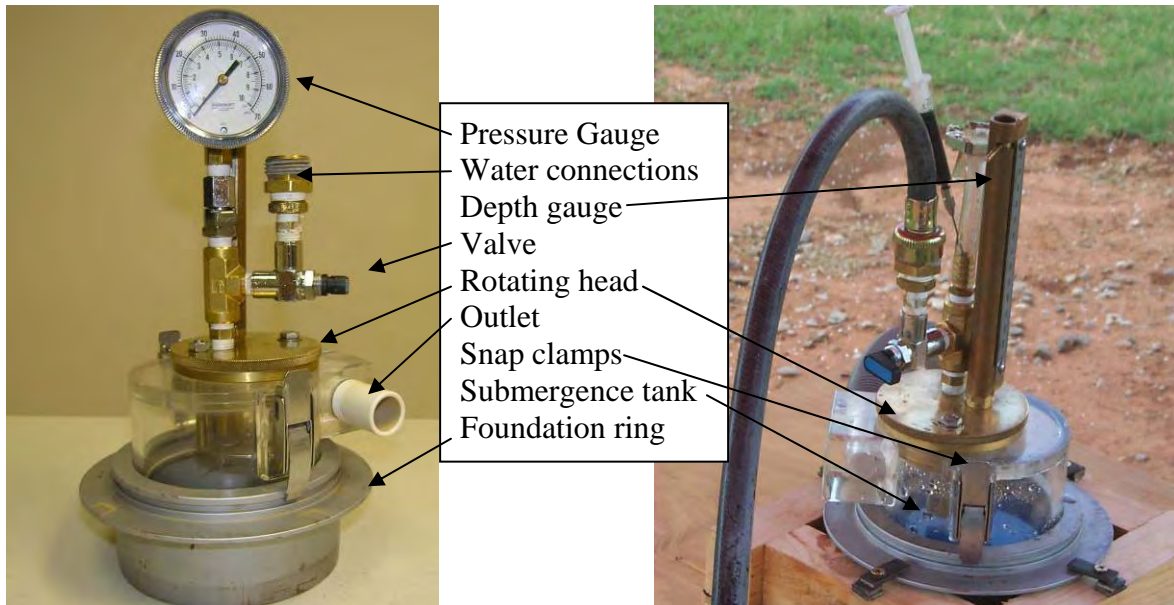


Figure 2 Mini-Jet (~0.12 m diameter) including foundation ring, submergence tank, rotating head, outlet, water delivery connections, gauge, valve, outlet, snap clamps, and depth gauge.

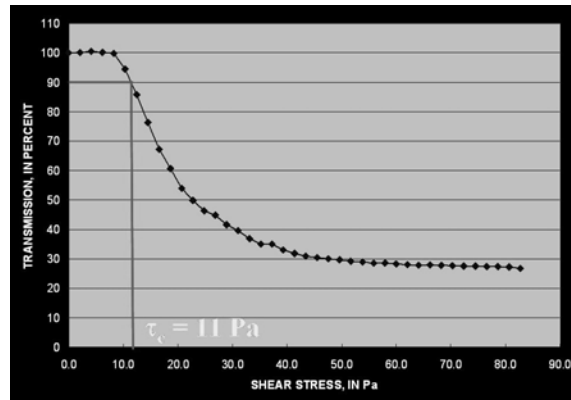


Figure 3 Photograph of CSM (left), and method of obtaining critical shear stress from relation between light transmission and applied shear stress (right).

Cohesive Strength Meter (CSM) As an alternative to the submerged jet-test device, a Cohesive Strength Meter (CSM; Tolhurst et al., 1999; Watts et al., 2003) was developed (Figure 3). The CSM is different to the submerged jet-test device in that it does not measure scour depth over time. Instead, there is an optical sensor within the sample head that measures light transmission through the water column as the test progresses. The shear stress corresponding to a reduction in light transmission to 90% of the starting value (which is usually near to 100%) is considered to indicate incipient motion of particles and thus represents the critical shear stress (τ_c) of the material being tested. As the eroded soil volume over time is not obtained with tests using the CSM, k cannot be calculated directly from the test results and must instead be calculated using, for example, a relation between τ_c and k determined from jet data.

RELATION BETWEEN CRITICAL SHEAR STRESS AND ERODIBILITY COEFFICIENT

Hanson and Simon (2001) described a relation between τ_c and k based on a total of 47 tests from western Iowa, eastern Nebraska and central Mississippi using the original jet-test device:

$$k = 0.2 \tau_c^{-0.5} \quad (3)$$

This relation has been updated with an additional 775 tests from 16 states across the country (Figure 4). Data scatter increases dramatically with decreasing τ_c to roughly 0.1 Pa. At τ_c less than 0.1 Pa, the relation breaks down and there is either (1) no discernable relation or (2) k attains a roughly constant, maximum value. This holds true for similar plots for each basin. For example, at τ_c less than 0.1 Pa (high excess shear stress), median k ranged from 0.28 $\text{cm}^3\text{N}^{-1}\text{s}^{-1}$ for the relatively resistant streambeds of the Yalobusha River, MS to 33.4 $\text{cm}^3\text{N}^{-1}\text{s}^{-1}$ for the sandier alluvium of the Upper Truckee River, CA. These findings imply that k does not vary by an inverse power function under conditions of very high excess shear stress (in the range of 100 to 1,000), but reaches a maximum value as a function of the nature of the eroding materials. This can be attributed to: (1) the mass erosion and/or (2) entrainment of fluid mud erosion mechanisms proposed by Mehta (1991). Because the general relation consistently breaks down at τ_c less than 0.1 Pa, computed $\tau_c - k$ relations were truncated at that point. This study shows that for this larger data set with the original jet device (702 tests; 120 tests removed) that the Blaisdell solution yields ($r^2 = 0.54$):

$$k = 1.42 \tau_c^{-0.824} \quad (4)$$

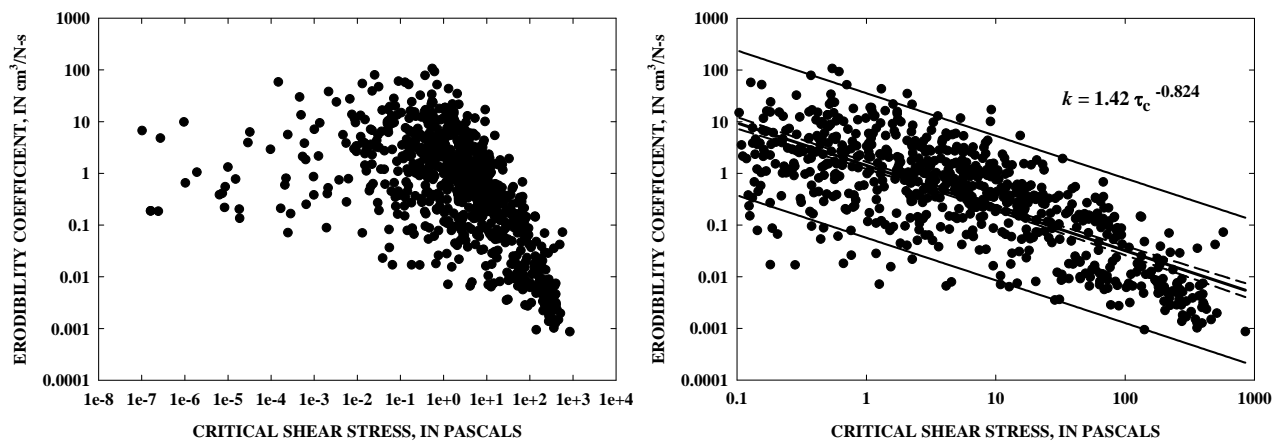


Figure 4 Data spread between τ_c and k based on 822 tests using the original (Hanson, 1990) jet-test device (left), and resulting regression relation for condition where $\tau_c \geq 0.10$ Pa (702 tests) (right). Dashed lines represent 95% confidence limits and the outer, solid lines represent 95% prediction limits.

Relations calculated for individual watersheds had exponents ranging from -0.11 to -1.0 and coefficients ranging from 0.25 to 6.1.

The relation predicting k from τ_c described by Equation 4 indicates that 46% of the variability is unexplained. Further, even in log-log space, the relation shows 95% prediction limits of greater than an order of magnitude on either side of the regression line (Figure 4, right). An analysis using data from 279 tests with the “mini” jet-test device produced very similar results but with even greater data scatter (Figure 5). The resulting equation for predicting k from τ_c using the “mini” jet-test device is ($r^2 = 0.42$; 203 tests):

$$k = 2.24 \tau_c^{-0.761} \quad (5)$$

and is not statistically different from Equation 4.

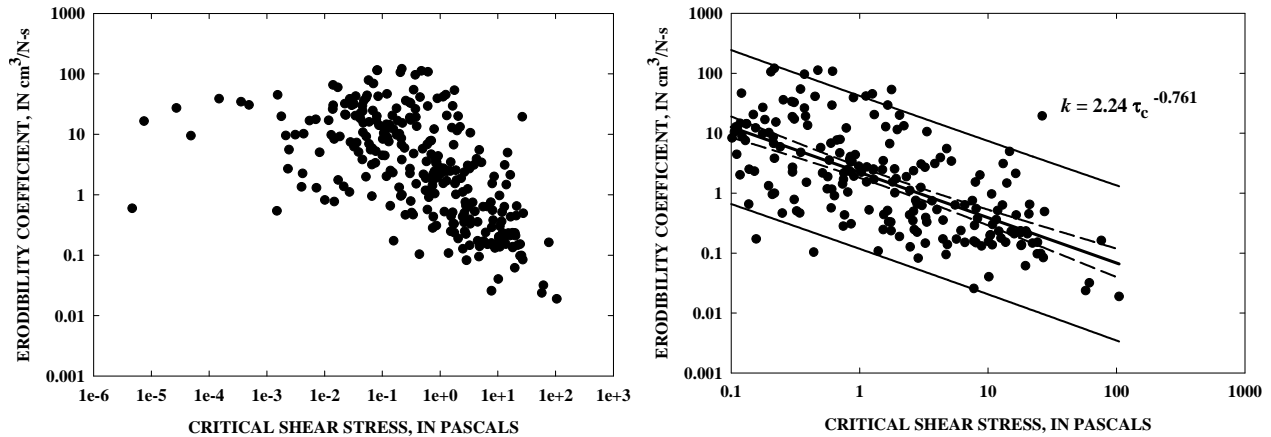


Figure 5 Data spread between τ_c and k based on 279 tests using the “mini” jet-test device (left), and resulting regression relation for condition where $\tau_c \geq 0.10$ Pa (203 tests) (right). Dashed lines represent 95% confidence limits and the outer, solid lines represent 95% prediction limits.

Combining all of the available jet-test data with $\tau_c > 0.0999$ Pa results in the following relation between k and τ_c ($r^2 = 0.62$):

$$k = 1.60 \tau_c^{-0.8264} \quad (5)$$

The effect of truncating the relation at $\tau_c = 0.1$ Pa is to increase the absolute value of the exponent by removing test data where low τ_c -values resulted in greater excess shear stresses. We propose several hypotheses to explain this large degree of uncertainty in predicting k from τ_c :

1. The erodibility coefficient (k), defined as the volume of material eroded per unit stress and time is not controlled by the entrainment threshold (τ_c) but by the geotechnical properties of the electrochemical bond between the cohesive particles. This was suggested earlier by Parchure and Mehta (1985) and Mehta (1991);
2. As the equilibrium scour depth is approached (and therefore, as the magnitude of the applied shear stress (τ_o) approaches τ_c of the bed material), the dominant factor in the erosion of the substrate is turbulent fluctuations and therefore erosion may continue, even though τ_o is computed to be less than τ_c (e.g. Robinson, 1989a, b; Stein et al., 1993); and
3. Calculations of τ_c and k using the Blaisdell solution method assume that the measured scour-time data can be modeled by a logarithmic-hyperbolic function (Hanson and Cook, 1997). This assumes that the time to reach the equilibrium scour depth is ∞ . The dimensionless time reached at the end of the test (T^*), defined below, is highly variable across the 1,100 tests. Results then are sensitive to the length of time the jet test is performed in the field. Further, in tests where the scour depth appears to have become asymptotic (i.e. equilibrium scour depth has been approached), this may cause τ_c to be under-predicted. This under-prediction is then propagated into the error-minimization routine employed to compute k , resulting in large root-mean-square errors and, therefore, potentially unreliable estimates of both τ_c and k .

To address hypothesis 3, two different, but complimentary, approaches have been developed to improve the reliability and reduce the uncertainty in the $\tau_c - k$ relations.

Effect of Data Filtering by Dimensionless Time (T^*) The Hanson and Cook (1997) methodology normalizes the measured scour depth using the predicted equilibrium scour depth (H_e) as the length scale, and normalizes the measured time using a reference time scale (T_r) defined by Stein et al. (1993) as:

$$T_r = H_e / (k \tau_c) \quad (6)$$

where H_e = equilibrium scour depth (m). The dimensionless time (T^*) is defined as (Stein et al., 1993; Hanson and Cook, 1997):

$$T^* = t / T_r \quad (7)$$

where t = time required to erode the bed from the nozzle tip to its ending elevation (s). Stein et al. (1993) stated that scour depth is within 95% of equilibrium when $T^* \geq 10$ and within 99.9% when $T^* \geq 100$. The significance of smaller values of T^* is a function of τ_o , the length of the jet potential core and the initial height of the nozzle above the bed. Larger values of T^* imply increased reliability of the Blaisdell curve-fitting procedure because this indicates that the test duration has neared the time theoretically required to reach equilibrium scour depth and hence, temporal extrapolation becomes more certain.

To test the idea that T^* could be used as a reliability indicator of τ_c and k -estimates, data from both the original and “mini” jet-test devices were combined and then filtered to retain only tests that had T^* -values exceeding a threshold value. Filtering by T^* was initiated at an extremely low value (0.0001; which included almost all of the data points) and then systematically increased to: (1) evaluate the progressive change in the $\tau_c - k$ relation with increasing T^* and (2) to determine a potentially optimum T^* value. For τ_c and k estimated using the Blaisdell solution, increasing T^* has the effect of increasing r^2 and the coefficient and reducing the value of the exponent in the $\tau_c - k$ relation (Table 1). A maximum r^2 value is reached at a T^* value of 0.25. Figure 6 compares the $\tau_c - k$ relations for all of the available data (left) and the data filtered so that only data with values of $T^* \geq 0.25$ are retained (right). Only 14% of the variability remains unexplained and the 95% prediction limits have been reduced to less than an order of magnitude on either side of the regression line (Figure 6, right).

Table 1 Impact of the non-dimensional time factor (T^*) on the coefficient and exponent in the $\tau_c - k$ relation.

T^*	Coefficient	Exponent	r^2
0.0001	1.60	-0.826	0.62
0.00025	1.80	-0.867	0.65
0.0005	1.98	-0.898	0.67
0.001	2.37	-0.948	0.7
0.0025	3.17	-1.038	0.73
0.005	4.32	-1.117	0.76
0.01	5.74	-1.187	0.78
0.025	9.13	-1.286	0.82
0.05	15.4	-1.401	0.83
0.1	25.7	-1.482	0.85
0.25	57.5	-1.601	0.86
0.5	130	-1.710	0.85
1	165	-1.630	0.81
2.5	3200	-1.942	0.86

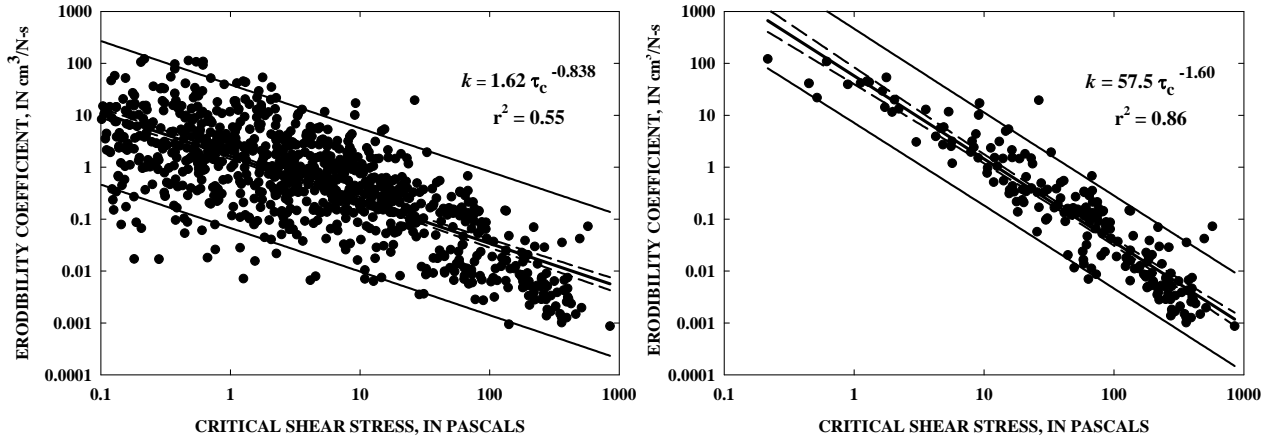


Figure 6 $\tau_c - k$ relation obtained using the Blaisdell solution based on 1,100 tests with both the original and “mini” jet-test devices for condition where $\tau_c \geq 0.10$ Pa (left) and resulting regression relation for condition where $T^* \geq 0.25$ Pa (199 tests) (right). Dashed lines represent 95% confidence limits and the outer, solid lines represent 95% prediction limits.

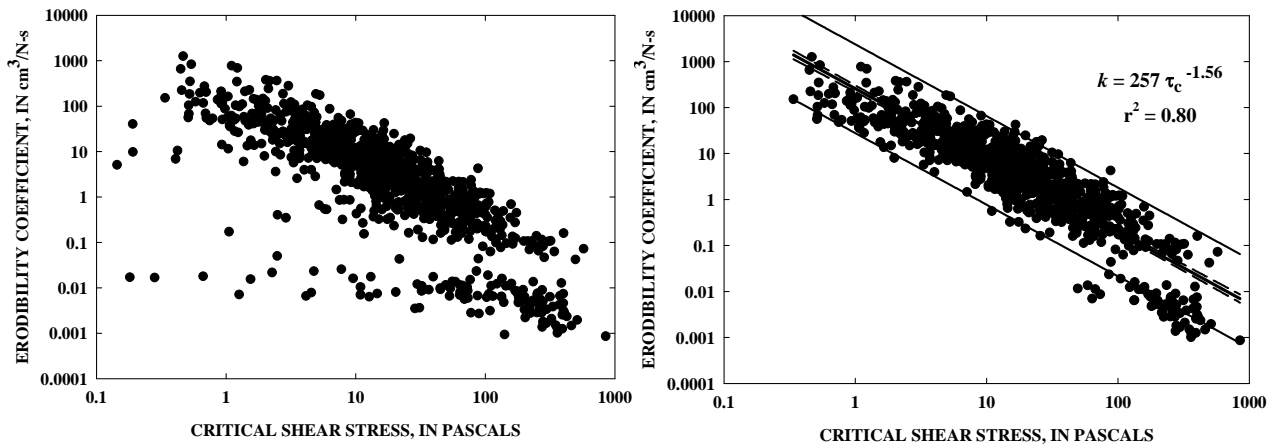


Figure 7 $\tau_c - k$ relation obtained using the Iterative solution based on 1,100 tests with both the original and “mini” jet-test devices for condition where $\tau_c \geq 0.10$ Pa (left) and resulting regression relation for condition where $T^* \geq 0.25$ Pa (936 tests) (right). Dashed lines represent 95% confidence limits and the outer, solid lines represent 95% prediction limits.

Preliminary analysis to improve understanding of T^* relative to non-dimensional scour depth (H^*) was performed to provide further justification of the use of T^* values such as $= 0.25$ as a reasonable data filter. The ratio of τ_c/τ_0 to the maximum possible τ_c value as defined within the Blaisdell solution can serve as a measure of the robustness of the solution. This maximum value is a function of the applied shear stress and two multipliers: (1) the depth of the potential core, and (2) the ratio of the nozzle diameter to the initial distance from the nozzle to the bed. The closer τ_c/τ_0 is to this maximum, the more uncertainty there is in the solution as it would take much longer testing periods to reach the equilibrium scour depth (note that for small ratios, the data collapse). For small ratios, however, the data collapse. For reasonable values of τ_c it was found that the non-dimensional scour depth (H^*) ranges from 70-75% of the equilibrium scour depth for values of T^* as low as 0.25 (Figure 8).

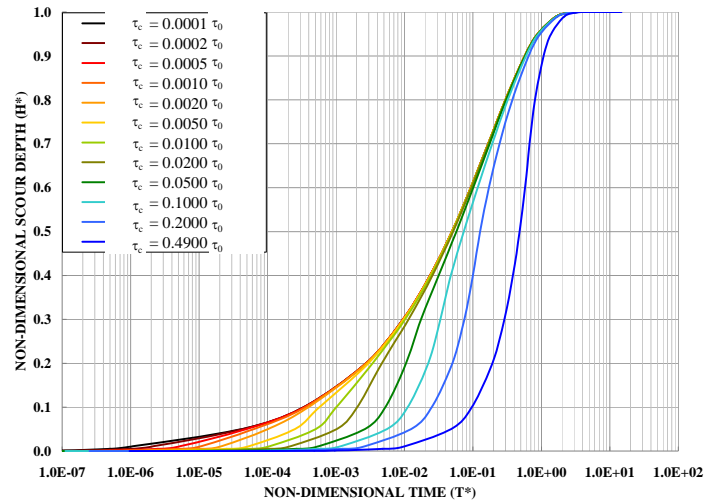


Figure 8 Solution for non-dimensional scour depth (H^*) as a function of non-dimensional time (T^*) for a range τ_c/τ_0 ratios showing (1) collapse of solutions for low values of the ratio, and (2) values of 0.70-0.75 (70-75%) of the equilibrium scour depth for $T^* = 0.25$.

Iterative Solution for τ_c and k An alternative solution has been developed to determine both τ_c and k from jet-scour data. This solution is based upon “Method 1” described in Hanson and Cook (1997), but with modification to improve the robustness of the solution. First, the solution is initialized with the τ_c - and k -values estimated using the Blaisdell solution. Second, an upper bound is computed for τ_c , to prevent the equilibrium scour depth from being exceeded. This upper bound is a function of the water pressure at the jet nozzle, the nozzle diameter and the maximum scour depth observed during the test. Third, a simultaneous solution that minimizes the root-mean-square error between the measured and predicted time is sought for both τ_c and k .

The results obtained after applying this solution are shown in Figure 7 (left). Compared with the Blaisdell solution (Figure 6; left), the scatter in the $\tau_c - k$ relation has been significantly reduced, with outliers appearing along a horizontal band at a k -value of approximately $0.01 \text{ cm}^3\text{N}^{-1}\text{s}^{-1}$. It is hypothesized that these values are a result of inappropriate temporal extrapolation because application of the $T^* \geq 0.25$ Pa filter removed these points (right). It is noted that the exponent is very similar to that obtained when the T^* filter was applied to the τ_c - and k -values estimated with the Blaisdell solution, although the coefficient is five times larger. The relation also becomes more negative at τ_c values greater than 100 Pa, implying that a power function may not be the most suitable function to describe the relation between τ_c and k .

Preliminary Validation Attempts at validating the iterative and Blaisdell solution methods for τ_c and k were conducted as part of a separate study on bank-retreat rates along the Upper Truckee River, CA (Simon and Thomas, 2009). Bank-toe erosion and associated mass failure of the upper part of the banks were simulated for a series of storm events that occurred over a year. Simulation results were then compared to measured erosion over the same period during which time one mass failure occurred by undercutting of the bank toe. Results showed that erosion was under-predicted using the original Hanson and Simon (2001) relation (Eq. 3) (zero mass failures) and over-predicted using the values from the iterative solution method (Figure 7, right) where three failures were predicted due to excessive undercutting. The best results were obtained using Equation 5, based on the Blaisdell solution and truncated at 0.1 Pa.

COMPARISON OF INSTRUMENTS: TUALATIN RIVER BASIN, OREGON

Collecting resistance and erodibility data of cohesive materials in the field is challenging and is generally conducted with two people. Testing requires the use of water on site and attempts to minimize the weight and volume of the instruments for ease in reaching remote field sites as well as testing in areas where space is limited. The original jet-test device (0.3 m-diameter) with its associated hoses, and gas-powered water pump was unwieldy and heavy. The “mini” jet device (0.15 m diameter), although lighter and requiring a smaller pump still required a gas-powered generator to operate the pump. In a continued effort to utilize a smaller and lighter instrument, the cohesive strength meter (CSM) was fit into a backpack and easily carried to remote sites. All three instruments were used at 35 sites in the Tualatin River Basin, Oregon to compare testing results.

Comparison between the three instruments was best accomplished by plotting the frequency distributions for all values of τ_c obtained in the field. The data set included 86 “mini” jet tests, 127 original jet tests and 129 CSM tests. Values of τ_c for the two jet-test devices show close agreement across most of the range of test values, with minor discrepancies at the tails of the distribution (Figure 9, left). Median values for the original and “mini” jets were 2.26 and 2.46 Pa, respectively; inter-quartile ranges were 8.43 and 8.14 Pa, respectively. The τ_c distribution for the CSM showed a much tighter distribution (median of 1.44 Pa; inter-quartile range of 1.27 Pa) but seems to be providing a completely different measure of incipient motion than the jet devices (Figure 9, left). Whereas results from the jet devices rely on tested hydraulic-diffusion principles of a submerged circular jet and the corresponding scour produced by the jet, the CSM relies on an empirical measurement of light transmission (or turbidity) to determine the point of incipient motion (τ_c). Although the CSM may be measuring a true initiation of motion, there are at several potential concerns with interpretation of its test results:

1. There is great uncertainty of the characteristics of the jet produced by the CSM, particularly with regard to turbulence and wall effects;
2. Erosion of material directly below the jet may be due to the direct impact of the jet rather than a circular shear-stress distribution created within the CSM’s cylinder;
3. The use of light transmission (or turbidity) as a measure of erosion is potentially problematic due to the presence of organics and other stains;
4. Experience gained by conducting more than one thousand field tests of τ_c across the United States, more than 340 in the Tualatin River Basin and applying these results to erosion-rate predictions indicate that the τ_c -values for many of the testing locations were most certainly much greater than 4.7 Pa (99th percentile value with the CSM); and
5. It is similarly difficult to accept that the resistance of all of the materials within the Tualatin River Basin fall within such a narrow range of corresponding particle diameters for non-cohesive materials (sand to fine-gravel range).

Predictions of k with the two jet devices (CSM cannot measure k) show parallel but distinctly different distributions, with the original jet device producing higher values of k across the entire range of tests (Figure 10, right). This is further supported by comparing the $\tau_c - k$ relations for the two devices where remarkably similar (parallel) regression slopes (-0.47) were produced (Figure 10). The difference lies in the regression coefficient which is 2.25 times greater for the original jet relation than for the mini-jet relation. We hypothesize that the differences in the k -distribution and $\tau_c - k$ relations may be due to differences in how the different-sized submerged jets diffuse and interact within their respective cans since the ratios of the circular areas of the jet can and jet are not identical. This hypothesis requires further testing and analysis.

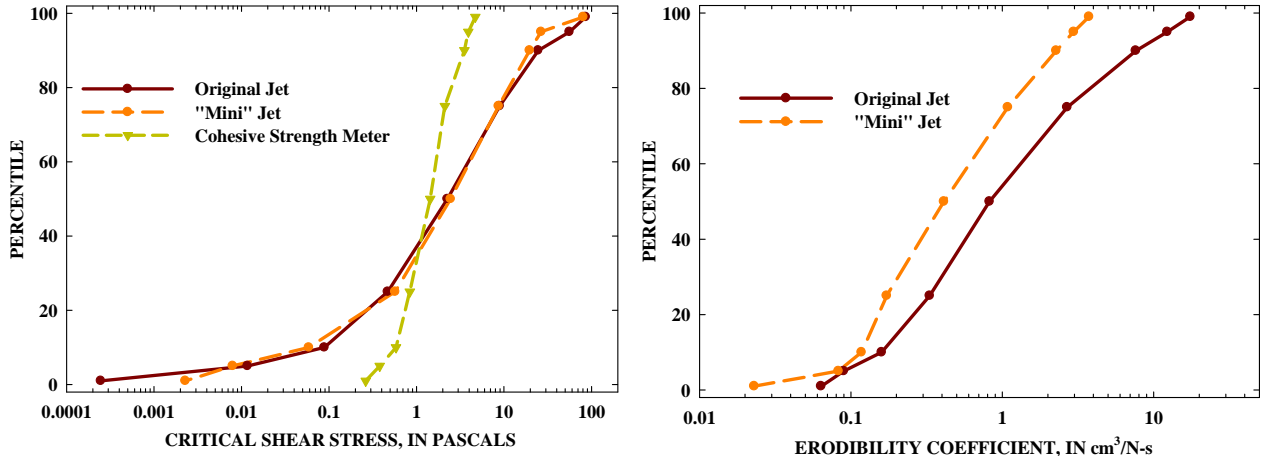


Figure 9 Distribution of τ_c -values for the original jet, “mini” jet, and CSM (left) and distributions of k for the two jet devices (right) in the Tualatin River Basin, Oregon.

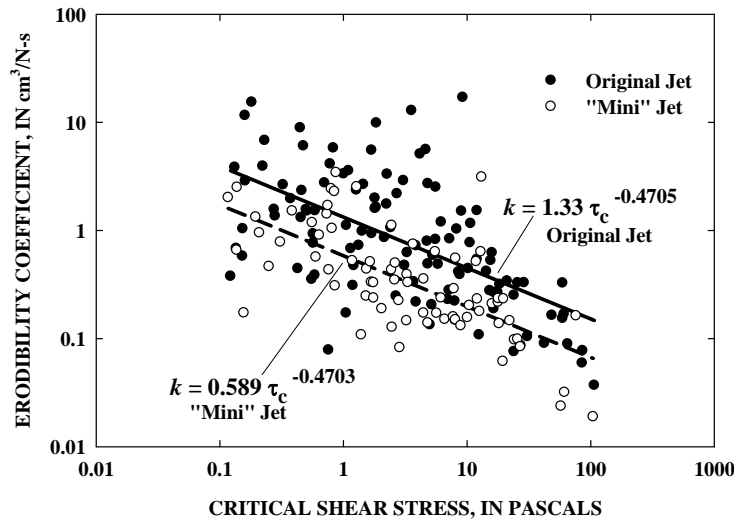


Figure 10 Relations between τ_c and k for original- and “mini”-jet tests in the Tualatin River Basin, Oregon. Note that the relations are parallel.

SUMMARY AND CONCLUSIONS

This study brings together data from about 1,100 jet tests and more than 200 tests with the cohesive strength meter (CSM). Results show that for each watershed tested, the general inverse-power form of the relation between τ_c and k were maintained. Data scatter increases dramatically with decreasing τ_c to roughly 0.1 Pa. At τ_c less than 0.1 Pa, the relation breaks down for all testing locations and there is either no defined relation or k attains a roughly constant, maximum value. These results imply that k does not vary by an inverse power function under conditions of very high excess shear stress but reaches a maximum value as defined by the bonding characteristics of the eroding materials. This maximum k -value, attained at high excess shear stresses for different tested basins ranged from less than 0.1 in basins with resistant clays to 33.4 $\text{cm}^3\text{N}^{-1}\text{s}^{-1}$ basins with the sandier alluvium. Relations calculated in this study were truncated at $\tau_c = 0.1$. Combining all available data in this way gives a steeper regression with a higher coefficient than the original relation published by (Hanson and Simon, 2001). This study shows

that $k = 1.6^{-0.826}$ ($r^2 = 0.62$). Data scatter, however, is still large with 95% prediction limits covering two orders of magnitude for a given τ_c .

Data were filtered by non-dimensional time (T^*) to reduce uncertainty in the relations by including only those tests that had attained a threshold value of the equilibrium scour depth. Filtering by a T^* -value of 0.25 was shown to produce the highest r^2 value, reduce uncertainty in prediction limits and represent 70-75% of the equilibrium scour depth over a range of critical shear stress to applied shear stress ratios.

Comparison of testing results between instruments in the Tualatin River Basin, Oregon disclosed that the two jet-test devices produced similar frequency distributions for τ_c over the range of testing materials. The CSM, however, produced a very different distribution corresponding to non-cohesive particle diameters in only the sand and fine-gravel range. It is hypothesized that this is probably due to the uncertainty in (1) the hydraulics imposed on the bed surface by the CSM, and (2) that incipient motion is defined as a measure of turbidity of the eroding fluid.

REFERENCES

- Ariathurai, R., and Arulanandan, K. (1978). "Erosion rates of cohesive soils," Journal of the Hydraulics Division, ASCE, 104(HY2), pp.279–283.
- Arulanandan, K. (1975). "Fundamental aspects of erosion of cohesive soils", Journal of the Hydraulics Division, ASCE, 101(HY5), pp.635–639.
- ASTM (1995). Annual Book of ASTM Standards: Section 4, Construction, v. 04-09. American Society for Testing and Materials, West Conshohocken, PA.
- Blaisdell, F.W., Clayton, L.A., and Hebaus, G.G. (1981). "Ultimate dimension of local scour," Journal of the Hydraulics Division, ASCE, 107(HY3), pp.327–337.
- Grissinger, E.H. (1982). Bank erosion of cohesive materials, In: R.D. Hey, J.C. Bathurst, and C.R. Thorne (eds.), Gravel-bed Rivers. John Wiley & Sons Ltd., Chichester, UK; pp.273–287.
- Hanson, G.J. (1990). "Surface erodibility of earthen channels at high stress, Part II - Developing an in situ testing device", Transactions ASAE, 33(1), pp.132–137.
- Hanson, G.J., and Cook, K.R. (1997). "Development of excess shear stress parameters for circular jet testing", American Society of Agricultural Engineers Paper No. 97-2227. American Society of Agricultural Engineers, St. Joseph, MO.
- Hanson, G.J., and Simon, A. (2001). "Erodibility of cohesive streambeds in the loess area of the midwestern USA", Hydrological Processes, 15(1), pp.23–38.
- Kelly, W.E., and Gularte, R.C. (1981). "Erosion resistance of cohesive soils, Journal of the Hydraulics Division, ASCE, 107(HY10), pp.1211–1223.
- Knighton, A.D. (1998). Fluvial Forms and Processes: A New Perspective. Arnold, London, UK.
- Mehta, A.J. (1991). Review notes on cohesive sediment erosion, In: N.C. Kraus, K.J. Gingerich, and D.L. Kriebel, (eds.), Coastal sediment '91, Proceedings of Specialty Conference on Quantitative Approaches to Coastal Sediment Processes, ASCE; pp.40–53.
- Parchure, T.M., and Mehta, A.J. (1985). "Erosion of soft cohesive sediment deposits", Journal of Hydraulic Engineering, ASCE, 110(10), pp.1308–1326.
- Partheniades, E. (1965). "Erosion and deposition of cohesive soils", Journal of the Hydraulics Division, ASCE, 91(HY1), pp.105–139.
- Robinson, K.M. (1989a). "Stress distribution at an overfall", Transactions ASAE, 32(1), pp.75–80.
- Robinson, K.M. (1989b). "Hydraulic stresses on an overfall boundary", Transactions ASAE, 32(4), pp.1269–1274.
- Shields, A. (1936). Application of similarity principles and turbulence research to bed-load movement. W.P. Ott, and J.C. van Uchelen (translators), Hydrodynamics Laboratory Publication 167. USDA

Soil Conservation Service Cooperative Laboratory, California Institute of Technology, Pasadena, CA.

- Simon, A. and Thomas, R.E. (2009). The fate of failed bank material and implications for lateral retreat: Lake Tahoe Basin, AGU Fall Meeting, San Francisco (Abs.), on CD.
- Stein, O.R., and Nett, D.D. (1997). "Impinging jet calibration of excess shear sediment detachment parameters", *Transactions ASAE*, 40(6), pp.1573–1580.
- Stein, O.R., Julien, P.Y., and Alonso, C.V. (1993). "Mechanics of jet scour downstream of a headcut", *Journal of Hydraulic Research*, 31(6), pp.723–738.
- Tolhurst, T.J., Black, K.S., Shayler, S.A., Mather, S., Black, I., Baker, K., and Paterson, D.M. (1999). Measuring the in situ Erosion Shear Stress of Intertidal Sediments with the Cohesive Strength Meter (CSM), *Estuarine, Coastal and Shelf Science*, 49(2), pp.281–294.
- Watts, C.W., Tolhurst, T.J., Black, K.S., and Whitmore, A.P. (2003). In situ measurements of erosion shear stress and geotechnical shear strength of the intertidal sediments of the experimental managed realignment scheme at Tollesbury, Essex, UK, *Estuarine, Coastal and Shelf Science*, 58(3), pp.611–620.
- Winterwerp, J.C. and van Kesteren, W.G.M. (2004). *Introduction to the Physics of Cohesive Sediment Dynamics in the Marine Environment*. Elsevier, Amsterdam.